

Photon-pion transition form factor: BABAR puzzle is cracked

A. E. Dorokhov

Joint Institute for Nuclear Research,

Bogoliubov Laboratory of Theoretical Physics,

141980 Dubna, Moscow region, Russian Federation;

Institute for Theoretical Problems of Microphysics,

Moscow State University, RU-119899, Moscow, Russian Federation

(Dated: November 9, 2018)

Abstract

Recently, the BABAR collaboration published (arXiv:0905.4778) data for the photon-pion transition form factor $F_{\pi\gamma\gamma^*}(Q^2)$, which are in strong contradiction to the predictions of the standard factorization approach to perturbative QCD. Immediately afterwards, two mechanisms were suggested (A.E. Dorokhov, arXiv:0905.4577; A.V. Radyushkin, arXiv:0906.0323), that logarithmically enhance the form factor asymptotics and therefore provide a qualitatively satisfactory description of the BABAR data. However, the physics of the BABAR effect was not fully clarified. In the present work, based on a nonperturbative approach to the QCD vacuum and on rather universal assumptions, we show that there exists two asymptotic regimes for the pion transition form factor. One regime with asymptotics $F_{\pi\gamma^*\gamma}(Q^2) \sim 1/Q^2$ corresponds to the result of the standard QCD factorization approach, while other violates the standard factorization and leads to asymptotic behavior as $F_{\pi\gamma^*\gamma}(Q^2) \sim \ln(Q^2)/Q^2$. Furthermore, considering specific nonlocal chiral quark models, we find the region of parameters, where the existing CELLO, CLEO and BABAR data for the pion transition form factor are successfully described.

I. INTRODUCTION

In the years 1977-1981, the theory of hard exclusive processes was formulated within the factorization approach to perturbative quantum chromodynamics (pQCD) [1–7]. The main ingredients of this approach are the operator product expansion (OPE), the factorization theorems, and the pQCD evolution equations. In this context, the form factor for the photon-pion transition $\gamma^*\gamma^* \rightarrow \pi^0$, with both photons being spacelike (with photon virtualities $Q_1^2, Q_2^2 > 0$), was considered in [6, 7]. Since only one hadron is involved, the corresponding form factor $F_{\pi\gamma^*\gamma^*}(Q_1^2, Q_2^2)$ has the simplest structure for the pQCD analysis among the hard exclusive processes. The nonperturbative information about the pion is accumulated in the pion distribution amplitude (DA) $\varphi_\pi(x)$ for the fraction x of the longitudinal pion momenta p , carried by a quark. Another simplification is, that the short-distance amplitude for the $\gamma^*\gamma^* \rightarrow \pi^0$ transition is, to leading order, just given by a single quark propagator. Finally, the photon-pion form factor is related to the axial anomaly [8, 9], when both photons are real.

Experimentally, the easiest situation is, when one photon virtuality is small and the other large. Under these conditions, the form factor $F_{\pi\gamma^*\gamma}(Q^2, 0)$ was measured at e^+e^- colliders by CELLO [10], CLEO [11] Collaborations (Fig. 1). In the region of large virtualities $Q^2 \gg 1 \text{ GeV}^2$, the pQCD factorization approach for exclusive processes predicts to leading order in the strong coupling constant [6, 7]

$$F_{\pi\gamma^*\gamma}^{\text{pQCD}}(Q^2, 0) = \frac{2f_\pi}{3Q^2} J, \quad (1)$$

where

$$J = \int_0^1 dx \frac{\varphi_\pi(x)}{x} \quad (2)$$

is the inverse moment of the pion DA, and $f_\pi = 92.4 \text{ MeV}$. The factor $1/Q^2$ reflects the asymptotic property of the quark propagator connecting two quark-photon vertices (Figs. 2a and 3). The formula (1) is derived under the assumption, that the QCD dynamics at large distances (the factor Jf_π) and the QCD dynamics at small distances (the factor $1/Q^2$) is factorized. Moreover, under this assumption, the asymptotics is reached already at the typical hadronic scale of a few GeV^2 . The pion DA $\varphi_\pi(x)$, in addition, evolves in shape with the change of the renormalization scale [4, 6] and asymptotically equals [3] $\varphi_\pi^{\text{As}}(x) = 6x(1-x)$. From this follows the famous asymptotic prediction (the short-dashed

line in Fig. 1)

$$F_{\pi\gamma^*\gamma}^{\text{pQCD,As}}(Q^2, 0) = \frac{2f_\pi}{Q^2}. \quad (3)$$

To describe the soft nonperturbative region of Q^2 , a simple interpolation between the $Q^2 \rightarrow 0$ and $Q^2 \rightarrow \infty$ limits has been proposed by Brodsky and Lepage (BL) (the dashed line in Fig. 1)

$$F_{\pi\gamma^*\gamma}^{\text{BL}}(Q^2, 0) = \frac{1}{4\pi^2 f_\pi} \frac{1}{1 + Q^2 / (8\pi^2 f_\pi^2)}. \quad (4)$$

Recently, the BABAR collaboration published new data (Fig. 1) for the $\gamma\gamma^* \rightarrow \pi^0$ transition form factor in the momentum transfer range from 4 to 40 GeV² [12]. They found the following puzzling result: At $Q^2 > 10$ GeV² the measured form factor multiplied by the photon virtuality $Q^2 F_{\pi\gamma^*\gamma}(Q^2, 0)$ exceeds the predicted asymptotic limit (3) and, moreover, continues to grow with increasing Q^2 . This result is in strong contradiction to the predictions of the standard QCD factorization approach mentioned above. The BABAR data very well match the older data obtained by the CLEO collaboration in the smaller Q^2 region, but extend to a much larger Q^2 values. There is numerous literature discussing the BABAR effect. We refer here only to the first two publications [13, 14] appeared soon after the data were announced and it is these works that are the most relevant for the following consideration. In these works two scenarios were suggested, that logarithmically enhance the form factor asymptotics and well describe the BABAR data.

The first scenario [13] uses the simple constituent quark model [15]. Within this model, the pion transition form factor, determined by the quark-loop (triangle) diagram with a momentum-independent quark mass M_q , is given by

$$F_{\pi\gamma\gamma^*}(Q^2, 0) = \frac{1}{4\pi^2 f_\pi} \frac{m_\pi^2}{m_\pi^2 + Q^2} \frac{1}{2 \arcsin^2(\frac{m_\pi}{2M_q})} \left\{ 2 \arcsin^2\left(\frac{m_\pi}{2M_q}\right) + \frac{1}{2} \ln^2 \frac{\beta_q + 1}{\beta_q - 1} \right\}, \quad (5)$$

where $\beta_q = \sqrt{1 + 4M_q^2/Q^2}$. The form factor (5) has correct normalization at zero photon virtualities, by the axial anomaly, and has double logarithmic asymptotics $\ln^2(Q^2/M_q^2)/Q^2$ at large Q^2 . This asymptotics corresponds to the case when large virtuality pass through all three quark propagators (Fig. 2c). In [13] it was shown that the pion transition form factor calculated from (5) with the parameter $M_q = 135$ MeV well reproduces the BABAR data. However, this model has serious shortcomings. Firstly, it has an incorrect chiral limit as $M_q \rightarrow 0$ and $m_\pi \rightarrow 0$. Secondly, the corresponding integral for the decay constant f_π within this quark model is divergent and thus the model should be regularized for consistency. After

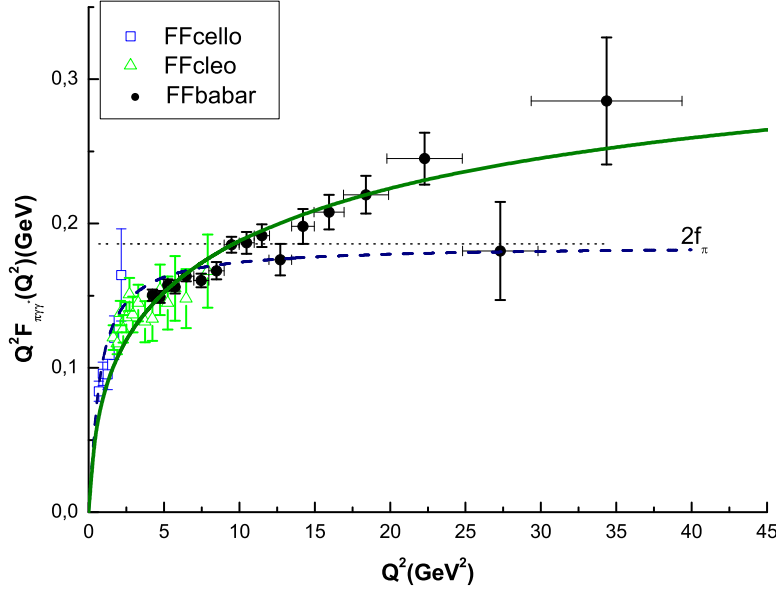


FIG. 1. The transition form factor $\gamma^*\gamma \rightarrow \pi^0$. The data are from the CELLO [10] (empty squares), CLEO [11] (empty triangles) and BABAR (filled circles) [12] Collaborations. The solid line is the model of this work, the dashed line is the Brodsky-Lepage prediction (4), the short-dashed line is massless QCD asymptotic limit (3).

regularization, however, the double logarithmic asymptotics is lost. Thirdly, just like in the Nambu–Jona-Lasinio model, it uses a local γ_5 vertex for the quark-pion vertex and the local quark propagator at all quark virtualities, in contradiction with pQCD, where there is no γ_5 operator, no pion as a bound state and no constituent quark mass. It is also well known, that in the local quark model the distribution amplitude and distribution function of the pion are constants [16–19].

Such flat (almost constant) pion DA was used in [14] in the context of the explanation of the BABAR data. The photon-pion transition form factor was calculated by using expression from [6] and incorporating a light-cone wave function $\Psi(x, k_\perp)$ that has rapid falloff with respect to the light-front energy combination $k_\perp^2/x(1-x)$. Within this approach, for a Gaussian shape of the light-cone wave function and assuming a flat pion DA $\varphi_\pi(x) = 1$, the pion transition form factor is given by

$$F_{\pi\gamma\gamma^*}^{\text{As}}(Q^2, 0) = \frac{2}{3} \frac{f_\pi}{Q^2} \int_0^1 \frac{dx}{x} \left[1 - \exp\left(-\frac{xQ^2}{2\sigma(1-x)}\right) \right], \quad (6)$$

and has logarithmically enhanced asymptotic behavior $\sim \ln(Q^2/2\sigma)/Q^2$. In [20] it was

demonstrated, that the descriptions of the BABAR data in the model (6) and in the model (5) practically coincide, if $\sigma = 0.48 \text{ GeV}^2$. In [14] it was also noted, that the use of such a wave function is numerically close to the leading-order pQCD expression for the photon-pion transition form factor with a modified quark propagator and a flat pion DA

$$F_{\pi\gamma\gamma^*}^{\text{As}}(Q^2, 0) = \frac{2}{3}f_\pi \int_0^1 \frac{dx}{xQ^2 + M^2}, \quad (7)$$

giving logarithmically enhanced asymptotics $F_{\pi\gamma\gamma^*}^{\text{As}}(Q^2, 0) \sim \ln(1 + Q^2/M^2)/Q^2$. With $M^2 = 0.6 \text{ GeV}^2$ the BABAR data are well fitted. Another very important feature of the scenario [14] is, that it was argued, that there is no pQCD evolution modifications in the shape of flat pion DA.

However, these approaches did not give an answer to the following serious questions. First of all, both expressions (6) and (7) do not describe the full form factor, but only the leading asymptotic part. They have incorrect normalization at $Q^2 = 0$, and are valid only at large photon virtuality $Q^2 \gg 1 \text{ GeV}^2$. Furthermore, the appearance of the parameter M in the asymptotic formula (7) is not justified. Moreover, as it was emphasized in [14], the expression (7) generates an infinite tower of false higher twist corrections $(M^2/xQ^2)^n$ in contradiction with OPE. It is well known [21], that there are only two terms in the OPE for the handbag diagram for the pion transition form factor: the twist-2 and the twist-4 terms. Also, the relation of the parameter σ in (6) or M in (7) to the fundamental QCD parameters and their values remained unclear. The decay constant f_π is external parameter in this approach and is not calculated dynamically. Finally, the origin of the flat DA is not well understood. Most of the QCD sum rule and the instanton model calculations lead to the endpoint suppressed amplitudes (see, e.g. [22, 23]). Below we show, how to generalize the results (5)-(7), and how to avoid the above mentioned problems with the interpretation of the BABAR data.

There are several QCD based approaches to treat the nonperturbative aspects of strong interactions. They are the lattice QCD, QCD sum rules, Schwinger–Dyson approach, Nambu–Jona-Lasinio model, etc. In the present paper, we analyze the photon-pion transition form factor in the gauged nonlocal chiral quark model based on the picture of nontrivial QCD vacuum. The attractive feature of this model is, that it interpolates the physics at large and small distances. At low energy, it enjoys the spontaneous breaking of chiral symmetry, the generation of the dynamical quark mass, and it satisfies the basic low energy theorems. At

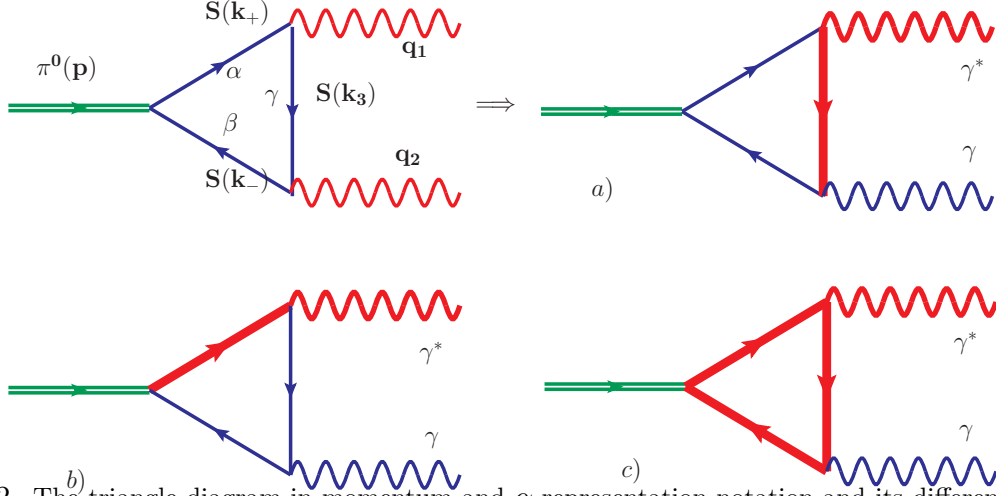


FIG. 2. The triangle diagram in momentum and α -representation notation and its different hard regimes for asymmetric kinematic. Hard photon is fat wavy line, real photon is thin wavy line; the fat line is the hard propagator, the thin line is the soft propagator: a) the standard factorization regime, b) the regime violating standard factorization, c) the double logarithmic regime with constant quark masses.

energies much higher than the characteristic hadronic scale, it becomes the theory of free massless quarks (in chiral limit).

The paper is organized as follows: In Sec. II, we give the basic elements of the effective chiral quark model, the quark propagator and the quark-photon and quark-pion vertices. In Sec. III, we transform the expression for the pion transition form factor into the α -representation and analyze, under rather general requirements on the nonperturbative dynamics, the asymptotic behavior of the form factor for different kinematics. Considering the kinematics when one photon is virtual and other is real, we show that two possible behaviors of the quark-pion vertex at large quark virtualities results in two different asymptotic regimes for the pion form factor. One of them corresponds to a standard factorized scheme with actual $1/Q^2$ asymptotics. The other provides a nonstandard asymptotic regime leading to $\sim \ln(Q^2)/Q^2$ large- Q^2 behavior of the pion form factor. In Sec. IV, we specify two kinds of nonlocal chiral quark model implementing different asymptotic regimes and obtain the pion DA for various sets of parameters. In Sec. V, we are looking for the space of parameters that give a satisfactory fit of the CELLO, CLEO and BABAR data. Sec. VI contains our conclusions.

II. NONLOCAL CHIRAL QUARK MODEL

Let us discuss the properties of the triangle diagram (Fig. 2) within the effective approach to nonperturbative QCD dynamics. To consider the asymptotics of the photon-pion transition form factor, we do not need to completely specify the elements of the diagram technique, which are, in general, model dependent, but shall restrict ourselves to rather general requirements. All expressions will be treated in Euclidean space appropriate for the nonperturbative physics. The nonperturbative quark propagator, dressed by the interaction with the QCD vacuum, is

$$S(k) = \frac{\widehat{k} + m(k^2)}{D(k^2)}. \quad (8)$$

The main requirement to the quark propagator is, that at large quark virtualities one has

$$S(k) \xrightarrow{k^2 \rightarrow \infty} \frac{\widehat{k}}{k^2}. \quad (9)$$

We assume also, that the dynamical quark mass is a function of the quark virtuality k^2 and normalized at zero as

$$m(0) = M_q, \quad D(0) = M_q^2. \quad (10)$$

At large virtualities, it drops to the current quark mass m_{curr} faster than any power of k^{-2} (see the discussion in [26])

$$m(k^2) \sim M_q \exp(-(k^2)^a) + m_{curr}, \quad a > 0. \quad (11)$$

This is, firstly, because the dynamical quark mass is directly related to the nonlocal quark condensate [18, 27] and, secondly, the quark propagators with powerlike dynamical mass induce false power corrections that are in contradiction to OPE. On the other hand, the dynamical quark mass (11) generates exponentially small corrections, invisible in the standard OPE. The direct instanton contributions provide a famous example of these exponential corrections in the QCD sum rules approach [28, 29]. The denominator in (8) at large virtualities is $D(k^2) \xrightarrow{k^2 \rightarrow \infty} k^2$ and the typical expression is

$$D(k^2) = k^2 + m^2(k). \quad (12)$$

It is well known (see, e.g., [30, 31]), that the change of the quark propagator leads to a modification of the quark-photon vertex in order to preserve the Ward-Takahashi identity

$$\Gamma_\mu(k, q, k' = k + q) = -ie_q [\gamma^\mu - \Delta \Gamma_\mu(k, q, k' = k + q)], \quad (13)$$

where the extra term guarantees the property

$$q_\mu \Gamma_\mu(k, q, k' = k + q) = S^{-1}(k') - S^{-1}(k). \quad (14)$$

The term $\Delta\Gamma_\mu(q)$ is not uniquely defined, even within a particular model, especially its transverse part. The importance of the full vertex Γ_μ is, that the axial anomaly is reproduced [32], and thus the photon-transition form factor correctly normalized. Fortunately, due to the fact, that $\Delta\Gamma_\mu$ is not proportional to γ_μ matrix, the corresponding amplitude has no projection onto the leading twist operator. Thus, this term is suppressed, if a large photon virtuality passes through the vertex, and hence does not participate in the leading asymptotics of the form factor. Its leading asymptotics results exclusively from the local part of the photon vertex

$$\Gamma_\mu^{\text{As}}(k, q, k' = k + q) = -ie_q \gamma^\mu. \quad (15)$$

Furthermore, we need the quark-pion vertex,

$$\Gamma_\pi^a(p) = \frac{i}{f_\pi} \gamma_5 \tau^a F(k_+^2, k_-^2), \quad (16)$$

where k_+ and k_- are the quark and antiquark momenta. It is important to note, that the quark-pion vertex function $F(k_+^2, k_-^2)$ plays a similar role in our consideration as the light-cone wave function $\Psi(x, k_\perp)$ in [1–7]. The vertex function $F(k_+^2, k_-^2)$ is symmetric in the quark virtualities k_+^2 and k_-^2 , and rapidly decreases, when both virtualities are large. If it were a function of a linear combination of the quark momenta k_+ and k_- , then it would led to a growing form factor with increasing spacelike photon momenta (see for discussions [23]). The spontaneous breaking of chiral symmetry ensures, that the vertex function $F(k_+^2, k_-^2)$ is a functional of the dynamical mass $m(k^2)$. In particular, the vertex function is normalized via

$$F(k^2, k^2) = m(k^2). \quad (17)$$

In the following, the important feature of the vertex function $F(k_+^2, k_-^2)$ will be its behavior in the limit, when one quark virtuality is asymptotically large and the other remains finite. There are two possibilities,

$$F^f(k_+^2, k_-^2) \xrightarrow{k_-^2 \rightarrow \infty} 0, \quad (18)$$

and

$$F^{uf}(k_+^2, k_-^2) \xrightarrow{k_-^2 \rightarrow \infty} g(k_+^2). \quad (19)$$

Finally, one needs the projection of the pion state onto the leading twist operator, see Fig. 3,

$$\Gamma_{\mu}^{5,\text{As}}(k, q, k' = k + q) = \gamma^{\mu} \gamma^5. \quad (20)$$

This projection is determined by the matrix element $\langle 0 | \bar{q} \gamma^{\mu} \gamma^5 \tau^a q | \pi^a(p) \rangle = -i2f_{\pi,\text{PS}}$, where the constant $f_{\pi,\text{PS}}$ is (here $m'(u) = dm(u)/du$)

$$f_{\pi,\text{PS}}^2 = \frac{N_c}{4\pi^2} \int_0^1 du \quad u \frac{F(u, u)}{D^2(u)} \left(m(u) - \frac{1}{2} u m'(u) \right), \quad (21)$$

which coincides with the square of the pion decay constant $f_{\pi,\text{PS}}$ in the so-called Pagels-Stokar form [33]. However note, that the physical pion decay constant, f_{π} , entering the pion vertex (16), is calculated by using the axial vertex corresponding to the conserved axial current $\Gamma_{\mu}^5(q)$. It turns out that the constant $f_{\pi,\text{PS}}$ and the physical decay constant f_{π} are not always identical. We return to this point in Sec. IV.

Thus, we emphasize again, that in order to analyze the asymptotic behavior of the pion transition form factor $F_{\pi\gamma^*\gamma^*}(Q_1^2, Q_2^2)$ by inspecting the triangular diagram, one needs to specify only very general properties of the transition, from soft to hard regimes of the quark-pion-photon dynamics encoded in (9), (15), (16) and (21). At the same time, the full dynamics (8), (13), (16) should guarantee the low energy theorems, in particular, the correct normalization of the form factor by the axial anomaly

$$F_{\pi\gamma\gamma}(0, 0) = 1/(4\pi^2 f_{\pi}), \quad (22)$$

and the Goldberger-Treiman relation, connecting the quark-pion coupling $g_{q\pi}$ and the dynamical quark mass M_q with the physical pion decay constant f_{π} : $f_{\pi} = M_q/g_{q\pi}$.

III. ASYMPTOTICS OF PION-PHOTON TRANSITION FORM FACTOR

The invariant amplitude for the process $\gamma^* \gamma^* \rightarrow \pi^0$ is given by

$$A(\gamma^*(q_1, \epsilon_1) \gamma^*(q_2, \epsilon_2) \rightarrow \pi^0(p)) = -ie^2 \varepsilon_{\mu\nu\rho\sigma} \epsilon_1^{\mu} \epsilon_2^{\nu} q_1^{\rho} q_2^{\sigma} F_{\pi\gamma^*\gamma^*}(-q_1^2, -q_2^2), \quad (23)$$

where ϵ_i^{μ} are the photon polarization vectors, $p^2 = m_{\pi}^2$, $q_1^2 = -Q_1^2$, $q_2^2 = -Q_2^2$. In the effective nonlocal quark-model considered above, one finds the contribution of the triangle diagram to the invariant amplitude [23],

$$A(p^2; q_1^2, q_2^2) = A^{\text{loc}}(p^2; q_1^2, q_2^2) + A^{\text{nonloc}}(p^2; q_1^2, q_2^2),$$

where the first term contains only local part of the photon vertices

$$A^{\text{loc}}(p^2; q_1^2, q_2^2) = -ie^2 \frac{N_c}{3f_\pi} \int \frac{d^4 k}{(2\pi)^4} F(-k_+^2, -k_-^2) \cdot \{tr[i\gamma_5 S(k_-) \hat{\epsilon}_2 S(k_+ - q_1)] \hat{\epsilon}_1 S(k_+) + (q_1 \leftrightarrow q_2; \epsilon_1 \leftrightarrow \epsilon_2)\}, \quad (24)$$

and the second term comprises the rest

$$A^{\text{nonloc}}(p^2; q_1^2, q_2^2) = -ie^2 \frac{N_c}{3f_\pi} \int \frac{d^4 k}{(2\pi)^4} F(-k_+^2, -k_-^2) \cdot \{tr[i\gamma_5 S(k_-) S(k_+ - q_1) \hat{\epsilon}_1 S(k_+)] (\epsilon_2, \Delta\Gamma(k_+, -q_1, k_+ - q_1)) + tr[i\gamma_5 S(k_-) \hat{\epsilon}_2 S(k_+ - q_1) S(k_+)] (\epsilon_1, \Delta\Gamma(k_+ - q_1, -q_2, k_-))\} + (q_1 \leftrightarrow q_2; \epsilon_1 \leftrightarrow \epsilon_2), \quad (25)$$

with $p = q_1 + q_2$, $q = q_1 - q_2$, $k_\pm = k \pm p/2$.

As we discussed above, the leading asymptotics results from the local part of the amplitude, A^{loc} . After taking the Dirac trace and going to Euclidian metric ($d^4 k \rightarrow id^4 k$, $k^2 \rightarrow -k^2$), one obtains

$$A^{\text{loc}}(p^2; q_1^2, q_2^2) = \frac{e^2 N_c}{6\pi^2 f_\pi} \int \frac{d^4 k}{\pi^2} F(k_+^2, k_-^2) \frac{m(k_+^2) (\varepsilon_{12kq_2} - \varepsilon_{12q_1q_2}) - m(k_-^2) \varepsilon_{12q_1k} + m(k_3^2) \varepsilon_{12pk}}{D(k_+^2) D(k_-^2) D(k_3^2)}, \quad (26)$$

where $k_3^2 = (k_+ - q_1)^2$, and $\varepsilon_{12kq_2} = \varepsilon_{\mu\nu\lambda\rho} \epsilon_1^\mu \epsilon_2^\nu k^\lambda q_2^\rho$, etc.

In order to analyze the asymptotic properties of the form factor, let us transform the integral in (26) formally into the α representation (see [34, 35]), which is one of the basic methods for the study of hard processes in perturbative QCD [36], as well as in nonperturbative quark models [18]. Let us define for any function F of virtuality k^2 , decaying at large virtuality as $1/k^2$ or faster, its α representation (Laplace transform)

$$F(k^2) = \int_0^\infty d\alpha e^{-\alpha k^2} f(\alpha), \quad F(k^2) \sim f(\alpha), \quad (27)$$

where $F(k^2)$ is the image of the original $f(\alpha)$. The important asymptotic property of this representation is, that the large power-like k^2 behavior of $F(k^2)$ is given by derivatives of the original $g(\alpha)$ at $\alpha = 0$

$$F(k^2) \stackrel{k^2 \rightarrow \infty}{\sim} \frac{f(0)}{k^2} + \frac{f'(0)}{k^4} + \frac{f''(0)}{k^6} + \dots \quad (28)$$

Thus, the large k^2 asymptotics of the image $F(k^2)$ is related to the small α behavior of the original $f(\alpha)$.

Let us introduce the following notations

$$\frac{1}{D(k^2)} \sim d(\alpha), \quad \frac{m(k^2)}{D(k^2)} \sim d_m(\alpha), \quad (29)$$

$$\frac{F(k_+^2, k_-^2)}{D(k_+^2) D(k_-^2)} \sim G(\alpha, \beta), \quad \frac{m(k_+^2) F(k_+^2, k_-^2)}{D(k_+^2) D(k_-^2)} \sim G_{m,0}(\alpha, \beta), \quad (30)$$

where in the second line the double α representation is implied. Because of the properties (9) and (11) one has

$$\begin{aligned} d(0) &= 1, d'(0) = 0, d''(0) = 0, \dots, \\ d_m(0) &= 0, d'_m(0) = 0, \dots \end{aligned}$$

With this notation, using the standard technique of the α representation ([34, 35]), the momentum integral in (26) is transformed into the following expression for the form factor

$$\begin{aligned} F_{\pi\gamma^*\gamma^*}^{\text{loc}}(p^2; Q_1^2, Q_2^2) &= \frac{N_c}{6\pi^2 f_\pi} \int \frac{d(\alpha\beta\gamma)}{\Delta^3} e^{-\frac{1}{\Delta}[-\alpha\beta p^2 + \gamma(\alpha Q_1^2 + \beta Q_2^2)]} \\ &\cdot [d(\gamma)(\alpha G_{m,0}(\alpha, \beta) + \beta G_{0,m}(\alpha, \beta)) + \gamma d_m(\gamma) G(\alpha, \beta)], \end{aligned} \quad (31)$$

where $\Delta = \alpha + \beta + \gamma$ and $\int d(\alpha\beta\gamma) \dots = \int_0^\infty d\alpha \int_0^\infty d\beta \int_0^\infty d\gamma \dots$

A. Symmetric kinematics

Let us first consider the symmetric kinematics $Q_1^2 = Q_2^2 = Q^2$. Then one has

$$\begin{aligned} F_{\pi\gamma^*\gamma^*}^{\text{loc}}(p^2; Q^2, Q^2) &= \frac{N_c}{6\pi^2 f_\pi} \int \frac{d(\alpha\beta\gamma)}{\Delta^3} e^{-\frac{1}{\Delta}[-\alpha\beta p^2 + \gamma(\alpha + \beta)Q^2]} \\ &\cdot [d(\gamma)(\alpha G_{m,0}(\alpha, \beta) + \beta G_{0,m}(\alpha, \beta)) + \gamma d_m(\gamma) G(\alpha, \beta)]. \end{aligned} \quad (32)$$

Large Q^2 behavior of $F_{\pi\gamma^*\gamma^*}^{\text{loc}}(p^2; Q^2, Q^2)$ corresponds to either small γ , small $\alpha + \beta$, or to large Δ . It is easy to check, that the leading asymptotics is ensured by small γ and thus $\Delta \rightarrow \alpha + \beta$. The term with factor $\gamma d_m(\gamma)$ provides only exponentially small corrections and does not contribute to the leading asymptotics. In this way, in (32), the integral over γ (small distances) and the integral over α, β (large distances) is factorized. The integral over γ , using (27), transforms the original $d(\gamma)$ back to momentum space $1/D(Q^2)$

$$F_{\pi\gamma^*\gamma^*}^{\text{loc}}(p^2; Q^2, Q^2) \stackrel{Q^2 \rightarrow \infty}{=} \frac{N_c}{6\pi^2 f_\pi} \frac{1}{D(Q^2)} \int \frac{d(\alpha\beta)}{(\alpha + \beta)^3} e^{\frac{\alpha\beta}{\alpha + \beta} p^2} (\alpha G_{m,0}(\alpha, \beta) + \beta G_{0,m}(\alpha, \beta)). \quad (33)$$

For the quark propagator, one obtains in this limit $1/D(Q^2) \rightarrow 1/Q^2$ plus exponentially small corrections, due to the properties (9) and (11). It turns out, that the integral in (33) is the α representation of the pion decay constant (21)

$$f_{\text{PS},\pi}^2 = \frac{N_c}{4\pi^2} \int \frac{d(\alpha\beta)}{(\alpha+\beta)^3} e^{\frac{\alpha\beta}{\alpha+\beta}p^2} (\alpha G_{m,0}(\alpha, \beta) + \beta G_{0,m}(\alpha, \beta)). \quad (34)$$

Thus one obtains the asymptotic formula

$$F_{\pi\gamma^*\gamma^*}^{\text{loc}}(0; Q^2, Q^2) \stackrel{Q^2 \rightarrow \infty}{=} \frac{2}{3} \frac{1}{Q^2} \frac{f_{\text{PS},\pi}^2}{f_\pi}, \quad (35)$$

for the form factor in symmetric kinematics, which for models, where $f_{\text{PS},\pi} = f_\pi$, reproduces the Brodsky-Lepage factorization result [7].

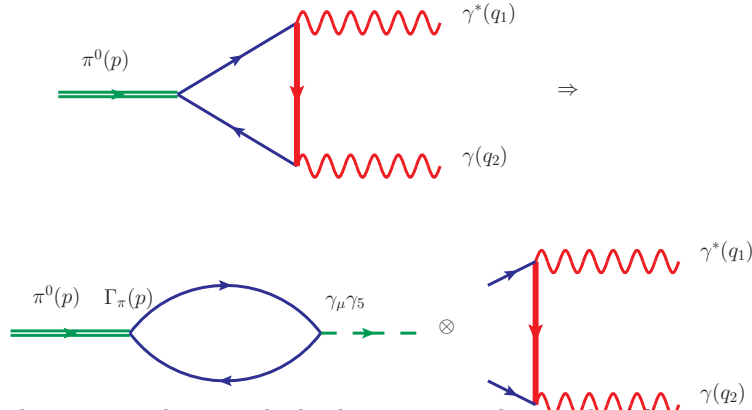


FIG. 3. At large photon virtualities in the leading twist, in the standard factorization regime, the amplitude is factorized into the soft pion matrix element and the hard coefficient function.

In order to define the pion DA, we carry out a change of variables in (34)

$$\alpha \rightarrow xL, \quad \beta \rightarrow \bar{x}L, \quad (36)$$

with $\bar{x} = (1 - x)$, then

$$\varphi_\pi(x) = \frac{N_c}{4\pi^2 f_{\text{PS},\pi}^2} \int_0^\infty \frac{dL}{L} e^{x\bar{x}Lp^2} (xG_{m,0}(xL, \bar{x}L) + \bar{x}G_{0,m}(xL, \bar{x}L)), \quad (37)$$

with

$$\int_0^1 dx \varphi_\pi(x) = 1.$$

In the momentum representation and using the chiral limit $p^2 = 0$, the result (37) for the leading twist DA is [23]

$$\varphi_\pi(x) = \frac{N_c}{4\pi^2 f_{\text{PS},\pi}^2} \int_{-\infty}^\infty \frac{d\lambda}{2\pi} \int_0^\infty du \frac{F(u + i\lambda\bar{x}, u - i\lambda x)}{D(u - i\lambda x) D(u + i\lambda\bar{x})} [xm(u + i\lambda\bar{x}) + \bar{x}m(u - i\lambda x)]. \quad (38)$$

This result is also in agreement with earlier calculations made in the instanton model under some simplified assumptions [19, 37–39]. The arguments in the integrand have the simple meaning of the transverse $u \equiv k_{\perp}^2$ and longitudinal parts of the quark (antiquark) virtualities.

For the pion vertex with the property (18), the pion DA vanishes at the endpoints

$$\varphi_{\pi}^f(x=0) = \varphi_{\pi}^f(x=1) = 0,$$

while for the second type of the pion vertex (19), one has instead

$$\varphi_{\pi}^{uf}(x=0) = \varphi_{\pi}^{uf}(x=1) = \frac{N_c}{4\pi^2 f_{\text{PS},\pi}^2} \int_0^\infty du \frac{m(u)g(u)}{D(u)}. \quad (39)$$

The pion DA $\varphi_{\pi}(x)$ in (37) is the leading twist-2 DA, defined as a gauge-invariant matrix element of the nonlocal operator

$$\left\langle 0 \left| \bar{d}(z) \gamma_{\mu} \gamma_5 P \exp \left(\int_{-z}^z dz^{\mu} A_{\mu}(z) \right) u(-z) \right| \pi^+(p) \right\rangle = i\sqrt{2} f_{\pi}^{\text{PS}} p_{\mu} \int_0^1 dx e^{i(2x-1)pz} \varphi_{\pi}(x), \quad (40)$$

with the Dirac structure $\gamma_{\mu} \gamma_5$ between the pion and vacuum states, z a light-like four-vector ($z^2 = 0$), and the gluon field $A_{\mu}(z)$.

Thus, in symmetric kinematics, the standard factorization is not violated and the OPE is modified only by exponentially small terms.

B. Asymmetric kinematics I

Let us now consider the asymmetric kinematics $Q_1^2 = Q^2, Q_2^2 = 0$. Then one has

$$F_{\pi\gamma^*\gamma}^{\text{loc}}(p^2; Q^2, 0) = \frac{N_c}{6\pi^2 f_{\pi}} \int \frac{d(\alpha\beta\gamma)}{\Delta^3} e^{-\frac{1}{\Delta}[-\alpha\beta p^2 + \gamma\alpha Q^2]} \cdot [d(\gamma)(\alpha G_{m,0}(\alpha, \beta) + \beta G_{0,m}(\alpha, \beta)) + \gamma d_m(\gamma) G(\alpha, \beta)]. \quad (41)$$

For simplicity in the following we shall consider the chiral limit, $m_{\text{curr}} = 0, p^2 = 0$.

Let us first consider the model with the quark-pion vertex possessing the property (18). In this case, the regime of small α does not lead to the leading asymptotic terms because of property $G(\alpha, \beta) \rightarrow 0$ as $\alpha \rightarrow 0$. The leading large Q^2 behavior corresponds to small γ , i.e. $\Delta \rightarrow \alpha + \beta$, (Fig. 2a), as for symmetric kinematics,

$$F_{\pi\gamma^*\gamma}^{\text{loc,I}}(0; Q^2, 0) \stackrel{Q^2 \rightarrow \infty}{=} \frac{N_c}{6\pi^2 f_{\pi}} \int \frac{d(\alpha\beta\gamma)}{(\alpha + \beta)^3} e^{-\frac{1}{\alpha + \beta} \gamma \alpha Q^2} d(\gamma)(\alpha G_{m,0}(\alpha, \beta) + \beta G_{0,m}(\alpha, \beta)). \quad (42)$$

This asymptotic term corresponds to the standard factorization contribution (Fig. 3) and the integral over γ again can be transformed back to the momentum space

$$F_{\pi\gamma^*\gamma}^{\text{loc,I}}(0; Q^2, 0) \stackrel{Q^2 \rightarrow \infty}{=} \frac{N_c}{6\pi^2 f_\pi} \int \frac{d(\alpha\beta)}{(\alpha + \beta)^3} \frac{\alpha G_{m,0}(\alpha, \beta) + \beta G_{0,m}(\alpha, \beta)}{D\left(\frac{\alpha Q^2}{\alpha + \beta}\right)}.$$

After change of variables (36), we arrive at the representation

$$F_{\pi\gamma^*\gamma}^{\text{loc,I}}(0; Q^2, 0) \stackrel{Q^2 \rightarrow \infty}{=} \frac{2}{3} \frac{f_{\text{PS},\pi}^2}{f_\pi} \int_0^1 dx \frac{1}{D(xQ^2)} \varphi_\pi^f(x), \quad (43)$$

where $\varphi_\pi(x)$ is defined in (37). Because in the considered case $\varphi_\pi(x)$ vanishes at the endpoints the actual asymptotics is

$$F_{\pi\gamma^*\gamma}^{\text{As,I}}(0; Q^2, 0) \stackrel{Q^2 \rightarrow \infty}{=} \frac{1}{Q^2} \frac{2}{3} \frac{f_{\text{PS},\pi}^2}{f_\pi} J^f \quad (44)$$

in agreement with (1), where $J^f = \int_0^1 \frac{dx}{x} \varphi_\pi^f(x)$ is given in the momentum space representation as [23]

$$J^f = \frac{N_c}{4\pi^2 f_{\text{PS},\pi}^2} \int_0^\infty du \frac{u}{D(u)} \int_0^1 dy \frac{F^f(u, yu) m(yu)}{D(yu)}. \quad (45)$$

As we have already noted in Introduction the asymptotic behavior (44) is not seen in the BABAR data. Nevertheless, even for the case considered, in principle, it is possible to simulate in some wide preasymptotic kinematical region a logarithmically enhanced behavior of the form factor. This happens if one assumes that the pion DA entering (43) is almost flat $\varphi_\pi(x) \approx 1$, i.e. it is close to a constant everywhere except small vicinity near endpoints. Then, in order to regularize the integral for J^f in the infrared region, one needs to keep the exponentially small terms in (43).

To this end, let us analyze the asymptotic behavior of the integral

$$J^L = Q^2 \int_0^1 dx \frac{1}{D(xQ^2)}, \quad (46)$$

corresponding to a flat pion DA, for some popular models of the nonperturbative quark propagator. Firstly, we consider the quark propagator

$$\frac{1}{D(k^2)} = \frac{1 - \exp(-k^2/\Lambda^2)}{k^2} \quad (47)$$

with the property of analytical confinement [40, 41]. In quark models, where this propagator is used, the parameter Λ has the meaning of a dynamical quark mass [42], $\Lambda \equiv M_q$, with typical values of $M_q = 200 - 300$ MeV. Inserting (47) into (46) one obtains

$$J_{AC}^L = \int_0^1 dx \frac{1 - \exp(-xQ^2/M_q^2)}{x} \quad (48)$$

with the leading asymptotic behavior

$$J_{AC}^L \stackrel{Q^2 \rightarrow \infty}{\simeq} \ln(Q^2/M_q^2) + \gamma_E, \quad (49)$$

where γ_E is the Euler-Mascheroni constant. Both expressions (48) and (49) are very close to the result (6) obtained in [14]. The difference is, that in the expression (48) the extra factor $(1-x)^{-1}$ in the exponent is absent, and more important the parameter in the exponent in (48) has clear physical sense as a dynamical quark mass squared.

Secondly, let us take the propagator of the general form given in (8)

$$J_Q^L = Q^2 \int_0^1 dx \frac{1}{xQ^2 + m^2(xQ^2)}. \quad (50)$$

Then one obtains the asymptotic behavior

$$J_Q^L \stackrel{Q^2 \rightarrow \infty}{\simeq} \ln(Q^2/M_q^2) + \int_0^\infty du \frac{M_q^2 - m^2(u)}{(u + m^2(u))(u + M_q^2)}. \quad (51)$$

Again, this is similar to (7) obtained in [14], but with important differences. In fact, (7) is a purely asymptotic formula and it is not allowed to keep the parameter M in the asymptotic quark propagator. The expression (50) is valid for all Q^2 and provides the leading asymptotics for the flat DA (51). It has correct large Q^2 behavior for the quark propagator, $1/Q^2$, and does not contain false power corrections.

C. Asymmetric kinematics II

Now, let us consider the model with the quark-pion vertex possessing the property (19). It is convenient to rearrange the terms in the pion form factor in the following way

$$\begin{aligned} F_{\pi\gamma^*\gamma}^{\text{loc,II}}(0; Q^2, 0) &= \frac{N_c}{6\pi^2 f_\pi} \int \frac{d(\alpha\beta\gamma)}{\Delta^3} e^{-\frac{\gamma\alpha}{\Delta} Q^2} \{ \beta r_m(\beta) \\ &+ \alpha G_{m,0}(\alpha, \beta) d(\gamma) + \beta [G_{0,m}(\alpha, \beta) - r_m(\beta)] \\ &+ \gamma G(\alpha, \beta) d_m(\gamma) + \beta r_m(\beta) [d(\gamma) - 1] \\ &+ \beta [d(\gamma) - 1] [\beta G_{0,m}(\alpha, \beta) - r_m(\beta)] \}, \end{aligned} \quad (52)$$

where we introduce notations for the originals

$$\frac{g(k^2)}{D(k^2)} \sim r(\alpha), \quad \frac{m(k^2)g(k^2)}{D(k^2)} \sim r_m(\alpha).$$

The term in the fourth line of (52) vanishes as $\gamma \rightarrow 0$ or $\alpha \rightarrow 0$, and thus does not participate in the leading asymptotics. The terms in the second line vanish as $\alpha \rightarrow 0$, but remains finite as $\gamma \rightarrow 0$. In this case, the $1/Q^2$ asymptotics is due to hard quark propagator connecting two photon vertices and the coefficient reflects the soft properties of the pion (Fig. 2a and Fig. 3). For the terms in the third line one has an opposite situation, they vanish with γ , but finite as $\alpha \rightarrow 0$. Thus, the $1/Q^2$ asymptotics is due to hard quark propagator connecting pion and hard photon vertices, while the coefficient correlates soft properties of the pion and photon (Fig. 2b and Fig. 4). The term in the first line of (52) provides the asymptotics $\sim \ln(Q^2)/Q^2$. This asymptotics corresponds to a combined soft-hard regime when one parameter (i.e. α) vanishes, while the other (γ) goes to infinity¹.

After standard manipulations with the integrals one obtains the following large- Q^2 asymptotic behavior transformed to the momentum representation

$$F_{\pi\gamma^*\gamma}^{As,\Pi}(0; Q^2, 0) \stackrel{Q^2 \rightarrow \infty}{=} \frac{1}{Q^2} \frac{N_c}{6\pi^2 f_\pi} \left[\int_0^\infty du \frac{m(u) g(u)}{D(u)} \ln\left(\frac{Q^2}{u}\right) + A \right], \quad (53)$$

$$A = \int_0^\infty du \frac{1}{D(u)} \int_0^1 dy \frac{m(yu)}{D(yu)} \{ u F^{uf}(u, yu) - [u + 2m^2(u)] g(yu) \}. \quad (54)$$

The coefficient of the logarithmic term in (53) is clearly related to the fact that the pion DA for the case considered does not vanish at the endpoints and proportional to the value of the pion DA at these points, see (39). When the function $g(u) \equiv 0$, we reproduce the asymptotics (44) and (45) corresponding to the quark pion vertex with property (18). The variable u in the integral (53) may be considered as the square of quark transverse momentum in the pion, $u \sim k_\perp^2$. The asymptotic expression (53) generalizes the asymptotic formula (1) for the case when the standard factorization is violated.

IV. THE INSTANTON AND CHIRAL MODELS

In the previous section we considered the asymptotic behavior of the pion transition form factor given in (23)-(25). In order to calculate this form factor in the whole kinematic region and compare with available experimental data, we should further specify our model assumptions. Let us introduce the momentum-dependent dynamical quark mass entering the propagator (8) as (we consider the chiral limit $m_{curr} = 0$)

$$m(k^2) = M_q f^2(k^2) \quad (55)$$

¹ See for classification of different regimes [36].

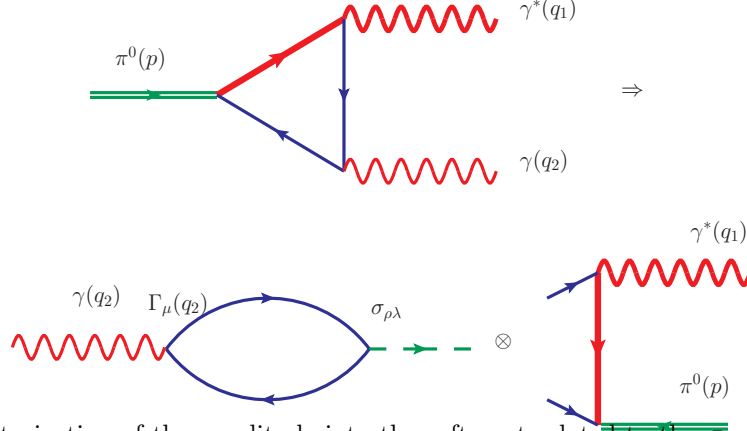


FIG. 4. The factorization of the amplitude into the soft part related to the $\sigma_{\mu\nu}$ projection of the photon wave function and the hard part of the quark propagator.

and take the profile function $f(k^2)$ in a Gaussian form

$$f(k^2) = \exp(-\Lambda k^2). \quad (56)$$

Thus, the model contains two parameters, the dynamical quark mass M_q and the non-locality parameter Λ .

Next, we need to specify the nonlocal part of the vector vertex that does not participate in the leading asymptotics, but is very important in implementing the low energy theorems. The nonlocal part of the vector vertex in (13) is taken of the form [30]

$$\Delta\Gamma_\mu(k, q, k' = k + q) = (k + k')_\mu \frac{m(k'^2) - m(k^2)}{k'^2 - k^2}. \quad (57)$$

Further, we will consider two kinds of quark-pion vertex (16), the first given by

$$F_I(k_+^2, k_-^2) = M_q f(k_+^2) f(k_-^2), \quad (58)$$

and the second by

$$F_\chi(k_+^2, k_-^2) = \frac{1}{2} M_q [f^2(k_+^2) + f^2(k_-^2)]. \quad (59)$$

The first one is motivated by the instanton picture of QCD vacuum [24] and the second by the nonlocal chiral quark model advertised in [25]. We shall in the further discussion refer to vertex function (58), which has the $k^2 \rightarrow \infty$ behavior (18), as the instanton model, and to the other choice (59), corresponding to $k^2 \rightarrow \infty$ behavior(19), as the chiral model.

The important requirement, that correlates the parameters of the models, is to fit the pion decay constant f_π . For the instanton based model this constant is given by the expression

found in [24]

$$f_{\text{DP},\pi}^2 = \frac{N_c}{4\pi^2} \int_0^\infty du \quad u \frac{m(u)}{D^2(u)} \left(m(u) - um'(u) + u^2 (m'(u))^2 \right), \quad (60)$$

and for the chiral model [25] the expression for f_π coincides with the Pagels-Stokar form (21). Within the nonlocal chiral model approach there is a difference between the vertex corresponding to the conserved axial current,

$$\Gamma_\mu^5(k, q, k' = k + q) = [\gamma^\mu \gamma^5 - \Delta \Gamma_\mu^5(k, q, k' = k + q)] \quad (61)$$

and the local vertex (20), corresponding to the leading twist operator. The total axial vertex $\Gamma_\mu^5(q)$ ensures the axial Ward-Takahashi identity and the Goldberger-Treiman relation. The nonlocal part of the axial vertex, that leads to (21) is given in [44] and to (60) is given in [31, 45, 46].

Fig. 5 shows the parameter space where the pion decay constant is fixed by its value taken in the chiral limit $f_\pi = 85$ MeV [47].

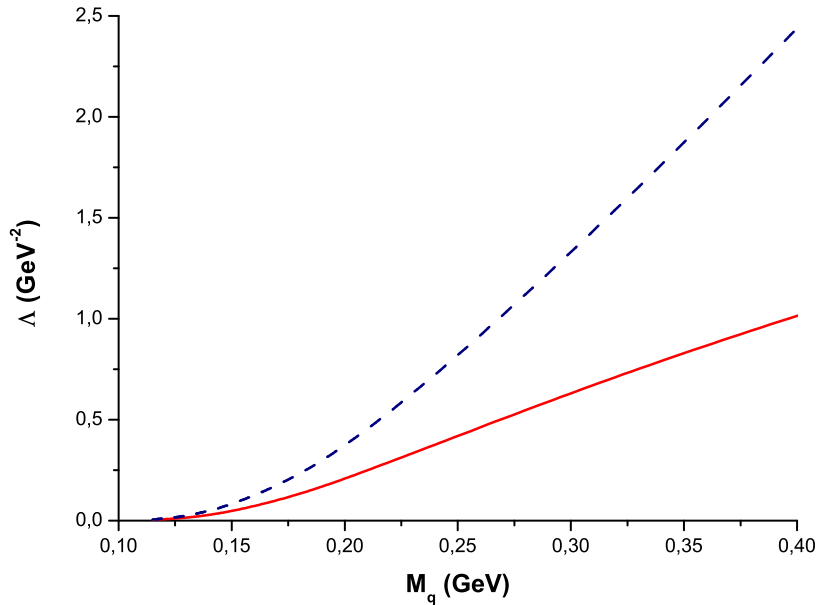


FIG. 5. The correlation between dynamical quark mass M_q and the nonlocal parameter Λ that fit the pion decay constant in chiral limit $f_\pi = 85$ MeV. The solid line is for the chiral model $f_{PS,\pi} = f_\pi$, and the dashed line is for the instanton model $f_{DP,\pi} = f_\pi$.

For the instanton model (58), the pion DA (37) is reduced to

$$\begin{aligned}\varphi_\pi^I(x) &= \frac{N_c}{4\pi^2 f_{\text{PS},\pi}^2} M_q \int_0^\infty \frac{dL}{L} (x\sigma_m(xL)\sigma(\bar{x}L) + \bar{x}\sigma(xL)\sigma_m(\bar{x}L)), \\ \varphi_\pi^I(x=0) &= 0, \quad \int_0^1 dx \varphi_\pi^I(x) = 1.\end{aligned}\tag{62}$$

For the chiral model (59), one obtains the pion DA

$$\varphi_\pi^\chi(x) = \frac{N_c}{8\pi^2 f_\pi^2} \int_0^\infty \frac{dL}{L} (x d_{m2}(xL) d(\bar{x}L) + \bar{x} d(xL) d_{m2}(\bar{x}L) + d_m(xL) d_m(\bar{x}L)), \tag{63}$$

$$\varphi_\pi^\chi(x=0) = \frac{N_c}{4\pi^2 f_\pi^2} \int_0^\infty du \frac{m^2(u)}{D(u)}, \quad \int_0^1 dx \varphi_\pi^\chi(x) = 1 \tag{64}$$

which is not vanishing at the endpoints $x=0$ and $x=1$.

In above expressions, we used the following notations for the correspondence between momentum and α -representation (in addition to definitions (29), (30))

$$\begin{aligned}\frac{m^2(k^2)}{D(k^2)} &\sim d_{m2}(\alpha), \\ \frac{f(k^2)}{D(k^2)} &\sim \sigma(\alpha), \quad \frac{m(k^2)f(k^2)}{D(k^2)} \sim \sigma_m(\alpha).\end{aligned}$$

The explicit form of the functions in α representation in the case of the model defined by (55) and (56) is given in Appendix.

In Fig. 6 the different shapes of the pion DA are shown as they are calculated within the instanton and chiral models for the values of the dynamical quark mass $M_q = 300$ MeV and $M_q = 125$ MeV. The parameter Λ is defined to fit the pion decay constant in chiral limit $f_\pi = 85$ MeV. For smaller M_q the pion DA is close to a flat shape. For larger M_q it is more sensitive to the nonlocal part of the photon vertex and, in case of the instanton model, it is strongly suppressed in the vicinity of endpoints.

In Fig. 7 the prediction for the pion transition form factor in symmetric kinematics calculated from (23)-(25) is presented. The explicit expression for the instanton model is

$$\begin{aligned}F_{\pi\gamma^*\gamma^*}^{\text{loc},I}(0; Q^2, Q^2) &= \frac{N_c M_q}{6\pi^2 f_\pi} \int \frac{d(\alpha\beta\gamma)}{\Delta^3} e^{-\frac{1}{\Delta}\gamma(\alpha+\beta)Q^2} \sigma(\beta) \\ &\cdot [2\alpha\sigma_m(\alpha)d(\gamma) + \gamma\sigma(\alpha)d_m(\gamma)],\end{aligned}\tag{65}$$

and for the chiral model is

$$\begin{aligned}F_{\pi\gamma^*\gamma^*}^{\text{loc},\chi}(0; Q^2, Q^2) &= \frac{N_c}{6\pi^2 f_\pi} \int \frac{d(\alpha\beta\gamma)}{\Delta^3} \alpha d(\gamma) \left[e^{-\frac{1}{\Delta}\gamma(\alpha+\beta)Q^2} d_{m2}(\alpha) d(\beta) \right. \\ &\quad \left. + \left(e^{-\frac{1}{\Delta}\gamma(\alpha+\beta)Q^2} + e^{-\frac{1}{\Delta}\alpha(\beta+\gamma)Q^2} \right) d_m(\alpha) d_m(\beta) \right].\end{aligned}\tag{66}$$

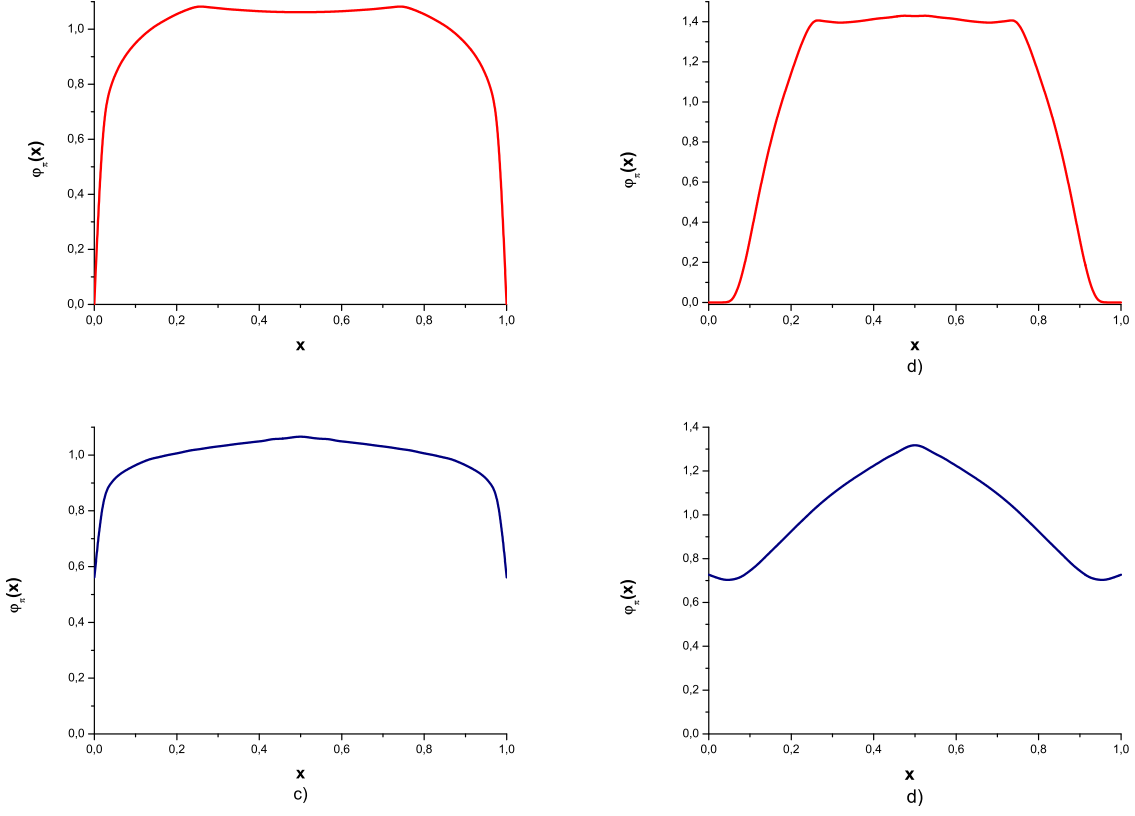


FIG. 6. Pion distribution amplitude for the instanton model with parameters a) $M_q = 125$ MeV, $\Lambda = 0.016$ GeV^{-2} and b) $M_q = 300$ MeV, $\Lambda = 1.3$ GeV^{-2} ; and chiral model with parameters c) $M_q = 125$ MeV, $\Lambda = 0.0098$ GeV^{-2} and d) $M_q = 300$ MeV, $\Lambda = 0.639$ GeV^{-2} .

As it is seen from Fig.7, the qualitative behavior of the pion transition form factor for fixed quark mass is similar for the two different models. For $M_q = 300$ MeV, the combination $Q^2 F_{\pi\gamma^*\gamma^*}$ rapidly turns into the asymptotic regime as expected in the standard factorization scheme. The asymptotic limits are different for the two models, $2f_\pi/3$ for the chiral model and $2f_{\text{PS},\pi}^2/3f_\pi$ for the instanton model. However, for smaller masses the effect of vertex non-localities is diminished, in particular $f_{DP,\pi} \approx f_{PS,\pi}$ for the instanton model. One sees from Fig. 7, that for $M_q = 125$ MeV the behavior of the form factors is similar for both models.

V. THE BABAR DATA WITHIN THE INSTANTON AND CHIRAL MODELS

Let us consider the model predictions for the pion transition form factor in the asymmetric kinematics ($q_1^2 = Q^2, q_2^2 = 0$) calculated from (23)-(25) in the region, where experimental

data exist. The explicit expression for the instanton model is

$$F_{\pi\gamma^*\gamma}^{\text{loc,I}}(0; Q^2, 0) = \frac{N_c M_q}{6\pi^2 f_\pi} \int \frac{d(\alpha\beta\gamma)}{\Delta^3} e^{-\frac{\alpha\gamma}{\Delta} Q^2} \cdot [(\alpha\sigma_m(\alpha)\sigma(\beta) + \beta\sigma(\alpha)\sigma_m(\beta))d(\gamma) + \gamma\sigma(\alpha)\sigma(\beta)d_m(\gamma)], \quad (67)$$

and for the chiral model is

$$F_{\pi\gamma^*\gamma}^{\text{loc,\chi}}(0; Q^2, 0) = \frac{N_c}{12\pi^2 f_\pi} \int \frac{d(\alpha\beta\gamma)}{\Delta^3} e^{-\frac{\alpha\gamma}{\Delta} Q^2} \{ \gamma d_m(\alpha) d(\beta) d_m(\gamma) + d(\gamma) [\alpha d_{m2}(\alpha) d(\beta) + d(\alpha) \beta d_{m2}(\beta) + (2\alpha + \beta) d_m(\alpha) d_m(\beta)] \}. \quad (68)$$

In Fig. 8, we show the predictions for different values of M_q . For a quark mass $M_q = 300$ MeV the model dependence is very strong and the theoretical curves are very far from the experimental points. The chiral model overshoots the data, while the instanton model, in correspondence with the standard factorization scenario, shows the asymptotic $1/Q^2$ behavior very early, already at $Q^2 \sim 1 \text{ GeV}^2$. It is clearly seen, that in order to describe the BABAR data, one has to take the dynamical quark mass $M_q \approx 125$ MeV. Then both models have an qualitatively good description, with some preference to the chiral model. In Figs. 9a and 10a we show that the parameter space that describes the data up to 40 GeV^2 is rather narrow. For the chiral model it is $M_q \approx 125 \pm 10$ MeV, and for the instanton model it is $M_q \approx 130 \pm 5$ MeV. Thus in this region the instanton model simulate the logarithmically enhanced behavior due to rather flat pion DA. However, the further behavior of the form factor is rather different for different models as it is seen in Figs. 9b and 10b, where the kinematical region up to 100 GeV^2 is shown. The instanton model finally reach its actual asymptotic $1/Q^2$ that follows from (44) and (45) with the asymptotic coefficient given by

$$J^I = \frac{N_c}{4\pi^2 f_{\text{PS},\pi}^2} M_q \int_0^\infty du \frac{uf(u)}{D(u)} \int_0^1 dy \frac{f(yu)m(yu)}{D(yu)} \quad (69)$$

For the chiral model the logarithmic growth continues for all Q^2 with the asymptotics following from (53)

$$F_{\pi\gamma^*\gamma}^{As,\chi}(0; Q^2, 0) \stackrel{Q^2 \rightarrow \infty}{=} \frac{1}{Q^2} \frac{N_c}{12\pi^2 f_\pi} \left[\int_0^\infty du \frac{m^2(u)}{D(u)} \ln\left(\frac{Q^2}{u}\right) + A^\chi \right], \quad (70)$$

$$A^\chi = \int_0^\infty du \frac{m(u)}{D(u)} \int_0^1 dy \frac{m(yu)}{D(yu)} [u - 2m(u)m(yu)].$$

Let us make few comments. First of all, the form factor and its asymptotics are rather different at lower Q^2 . From Fig. 11 it is seen that the asymptotic curve conjugates the calculated curve in the region of order of 100 GeV^2 . Secondly, the fact, that the quark mass leading to a satisfactory fit of the data is quite small, is not fully unexpected. There are not many quantities that are very sensitive to the dynamical quark mass. The precisely known contribution of the hadronic vacuum to the anomalous magnetic moment of muon, $g - 2$, is infrared sensitive and demands low values for the quark mass, $M_q \approx 200 \text{ MeV}$ [48–50]. Finally, remember also, that understanding the asymptotics of the pion transition form factor is important for selection of realistic nonperturbative models, used to estimate the hadronic contribution of the light-by-light process to $g - 2$ [51, 52].

VI. CONCLUSIONS

The present paper is devoted to the so-called BABAR puzzle. New very precise data were obtained by the BABAR collaboration for the photon-pion transition form factor in very wide kinematical region up to large photon virtualities $Q^2 \approx 40 \text{ GeV}^2$ [12]. The data overshoot the asymptotic limit for $Q^2 F_{\pi\gamma\gamma^*}(Q^2)$ predicted by Brodsky and Lepage [7], and have a tendency to grow further. Both facts are in strong contradiction with the standard QCD factorization approach, which constitutes the BABAR puzzle.

The main problem is the unstopped growth of the new data points for $Q^2 F_{\pi\gamma\gamma^*}(Q^2)$ that is inconsistent with the predicted $Q^2 F_{\pi\gamma\gamma^*}(Q^2) \rightarrow \text{constant}$, following from simple asymptotic properties of the massless quark propagator. The key point, to solve this problem, is to consider the properties of the pion vertex function $F(k_1^2, k_2^2)$ which is the analog of the light-cone pion wave function. There are two possibilities for the momentum dependence of the pion vertex function. In the limit, when one quark virtuality, k_1^2 , goes to infinity, and the other, k_2^2 , remains finite, the vertex function may not necessarily tend to zero. When it goes to zero, the pion DA $\varphi_\pi(x)$, which is a functional of the pion vertex function, is zero at the endpoints, $\varphi_\pi(0) = \varphi_\pi(1) = 0$, with either strong or weak suppression in the neighborhood of the endpoints $x = 0$ and $x = 1$. For the situation of strong suppression, the asymptotic $1/Q^2$ behavior of the pion form factor in asymmetric kinematics ($Q_1^2 = Q^2, Q_2^2 = 0$) is developed very early, in contradiction with the BABAR data. For weak suppression (resembling a flat distribution amplitude of the pion), the asymptotic $1/Q^2$ behavior is developed quite late,

and can give a reasonable description of the data in the BABAR region with a $\ln Q^2/Q^2$ behavior in this region. For the other case of non-vanishing pion vertex function in the above limit, the pion DA $\varphi_\pi(x)$ is not zero at the endpoints, and therefore the asymptotic $\ln Q^2/Q^2$ behavior persists over the whole range, in particular in the BABAR region.

In order to fit the available data on the photon-pion transition form factor from CELLO, CLEO and BABAR, we have analyzed the parameter space of two examples of nonperturbative models, motivated by the instanton [24] and the chiral [25] models, characterized by the two parameters, dynamical quark mass M_q and the parameter of non-locality Λ . The main conclusion is, that the fit to the data requires a quite small dynamical quark mass $M_q \approx 125$ MeV with rather small uncertainty. As a consequence, the parameter of non-locality, that fits the pion decay constant f_π , is very small, $\Lambda \sim 0.01 \text{ GeV}^{-2}$. Thus, one has an almost local quark model with very flat regulators in momentum space, that considerably diminishes the difference between the nonperturbative models considered in this work. In this respect, this situation resembles the fit by a simple local quark model, made in [13] with $M_q = 135$ MeV. On the other hand, in [14] only the leading asymptotics were used and large mass parameter of order of 1 GeV were required, to fit the BABAR data.

Finally we would like to point out, that in the present work, we did not consider QCD evolution. In [14], it was argued, that the flat pion DA corresponds to a very small momentum scale, and hence QCD evolution is frozen. Our calculations support this point of view. In particular, our choice of parameters fitting the BABAR data leads to quite large values of the quark condensate, also corresponding to a very low normalization point.

Concluding we may say, that the BABAR data being unique in their accuracy and covering a very wide kinematical range, are consistent with considerations based on nonperturbative QCD dynamics and may indicate specific properties of the pion wave function.

VII. ACKNOWLEDGMENTS

The author especially thanks S.V. Mikhailov and A.V. Radyushkin, and also W. Bro-niowski, S.B. Gerasimov, S.I. Eidelman, M.A. Ivanov, N.I. Kochelev, E.A. Kuraev, H.-P. Pavel, A.A. Pivovarov, A.E. Radzhabov for discussions on the interpretation of the high momentum transfer BABAR data for the pseudoscalar meson transition form factors. The author acknowledges partial support from the Scientific School grant 4476.2006.2 and the

VIII. APPENDIX

Here, the explicit expressions of the functions in α representation for the Gaussian model defined by (55) and (56) are given

$$\begin{aligned}
 d(\alpha) &= 1 + \sum_{n=1}^{\infty} \frac{(-1)^n}{n!} [M_q^2(\alpha - 4\Lambda n)]^n \Theta(\alpha - 4\Lambda n), \\
 d_m(\alpha) &= M_q \sum_{n=0}^{\infty} \frac{(-1)^n}{n!} [M_q^2(\alpha - \Lambda(2 + 4n))]^n \Theta(\alpha - \Lambda(2 + 4n)), \\
 d_{m2}(\alpha) &= M_q^2 \sum_{n=0}^{\infty} \frac{(-1)^n}{n!} [M_q^2(\alpha - \Lambda(4 + 4n))]^n \Theta(\alpha - \Lambda(4 + 4n)), \\
 \sigma(\alpha) &= \sum_{n=0}^{\infty} \frac{(-1)^n}{n!} [M_q^2(\alpha - \Lambda(1 + 4n))]^n \Theta(\alpha - \Lambda(1 + 4n)), \\
 \sigma_m(\alpha) &= M_q \sum_{n=0}^{\infty} \frac{(-1)^n}{n!} [M_q^2(\alpha - \Lambda(3 + 4n))]^n \Theta(\alpha - \Lambda(3 + 4n)).
 \end{aligned}$$

- [1] A. V. Radyushkin, (1977), hep-ph/0410276.
- [2] G. P. Lepage and S. J. Brodsky, Phys. Lett. **B87**, 359 (1979).
- [3] A. V. Efremov and A. V. Radyushkin, Theor. Math. Phys. **42**, 97 (1980).
- [4] A. V. Efremov and A. V. Radyushkin, Phys. Lett. **B94**, 245 (1980).
- [5] A. V. Efremov and A. V. Radyushkin, Submitted to 19th Int. Conf. on High Energy Physics, Tokyo, Japan, Aug 23-30, 1978.
- [6] G. P. Lepage and S. J. Brodsky, Phys. Rev. **D22**, 2157 (1980).
- [7] S. J. Brodsky and G. P. Lepage, Phys. Rev. **D24**, 1808 (1981).
- [8] S. L. Adler, Phys. Rev. **177**, 2426 (1969).
- [9] J. S. Bell and R. Jackiw, Nuovo Cim. **A60**, 47 (1969).
- [10] CELLO, H. J. Behrend *et al.*, Z. Phys. **C49**, 401 (1991).
- [11] CLEO, J. Gronberg *et al.*, Phys. Rev. **D57**, 33 (1998), hep-ex/9707031.
- [12] The BABAR, B. Aubert *et al.*, Phys. Rev. **D80**, 052002 (2009), 0905.4778.
- [13] A. E. Dorokhov, (2009), 0905.4577.

- [14] A. V. Radyushkin, Phys. Rev. **D80**, 094009 (2009), 0906.0323.
- [15] L. Ametller, L. Bergstrom, A. Bramon, and E. Masso, Nucl. Phys. **B228**, 301 (1983).
- [16] R. M. Davidson and E. Ruiz Arriola, Phys. Lett. **B348**, 163 (1995).
- [17] E. Ruiz Arriola and W. Broniowski, Phys. Rev. **D66**, 094016 (2002), hep-ph/0207266.
- [18] A. E. Dorokhov and L. Tomio, Phys. Rev. **D62**, 014016 (2000).
- [19] I. V. Anikin, A. E. Dorokhov, and L. Tomio, Phys. Lett. **B475**, 361 (2000), hep-ph/9909368.
- [20] A. E. Dorokhov, Nucl. Phys. Proc. Suppl. **198**, 190193 (2010), 0909.5111.
- [21] I. V. Musatov and A. V. Radyushkin, Phys. Rev. **D56**, 2713 (1997), hep-ph/9702443.
- [22] A. P. Bakulev, S. V. Mikhailov, and N. G. Stefanis, Phys. Rev. **D67**, 074012 (2003), hep-ph/0212250.
- [23] A. E. Dorokhov, JETP Lett. **77**, 63 (2003), hep-ph/0212156.
- [24] D. Diakonov and V. Y. Petrov, Nucl. Phys. **B272**, 457 (1986).
- [25] B. Holdom, J. Terning, and K. Verbeek, Phys. Lett. **B245**, 612 (1990).
- [26] A. E. Dorokhov, Eur. Phys. J. **C42**, 309 (2005), hep-ph/0505007.
- [27] A. E. Dorokhov, S. V. Esaibegian, and S. V. Mikhailov, Phys. Rev. **D56**, 4062 (1997), hep-ph/9702417.
- [28] E. V. Shuryak, Nucl. Phys. **B214**, 237 (1983).
- [29] A. E. Dorokhov and N. I. Kochelev, Z. Phys. **C46**, 281 (1990).
- [30] J. Terning, Phys. Rev. **D44**, 887 (1991).
- [31] R. D. Bowler and M. C. Birse, Nucl. Phys. **A582**, 655 (1995), hep-ph/9407336.
- [32] R. S. Plant and M. C. Birse, Nucl. Phys. **A703**, 717 (2002), hep-ph/0007340.
- [33] H. Pagels and S. Stokar, Phys. Rev. **D20**, 2947 (1979).
- [34] N. N. Bogolyubov and D. V. Shirkov, (Wiley, New York, 1980).
- [35] O. I. Zavialov, (Kluwer Academic, Dordrecht, 1990).
- [36] A. V. Radyushkin, Phys. Rev. **D56**, 5524 (1997), hep-ph/9704207.
- [37] S. V. Esaibegian and S. N. Tamarian, Sov. J. Nucl. Phys. **51**, 310 (1990).
- [38] A. E. Dorokhov, Nuovo Cim. **A109**, 391 (1996).
- [39] V. Y. Petrov, M. V. Polyakov, R. Ruskov, C. Weiss, and K. Goeke, Phys. Rev. **D59**, 114018 (1999), hep-ph/9807229.
- [40] G. V. Efimov and M. A. Ivanov, Int. J. Mod. Phys. **A4**, 2031 (1989).

- [41] G. V. Efimov and M. A. Ivanov, *The Quark Confinement Model of Hadrons* (, 1993), Bristol, UK: IOP, 177 p.
- [42] A. E. Radzhabov and M. K. Volkov, Eur. Phys. J. **A19**, 139 (2004), hep-ph/0305272.
- [43] A. E. Dorokhov, W. Broniowski, and E. Ruiz Arriola, Phys. Rev. **D74**, 054023 (2006), hep-ph/0607171.
- [44] B. Holdom, Phys. Rev. **D45**, 2534 (1992).
- [45] I. V. Anikin, A. E. Dorokhov, and L. Tomio, Phys. Part. Nucl. **31**, 509 (2000).
- [46] A. E. Dorokhov and W. Broniowski, Eur. Phys. J. **C32**, 79 (2003), hep-ph/0305037.
- [47] J. Gasser and H. Leutwyler, Nucl. Phys. **B250**, 465 (1985).
- [48] K. A. Milton, I. L. Solovtsov, and O. P. Solovtsova, Phys. Rev. **D64**, 016005 (2001), hep-ph/0102254.
- [49] A. A. Pivovarov, Phys. Atom. Nucl. **66**, 902 (2003), hep-ph/0110248.
- [50] A. E. Dorokhov, Phys. Rev. **D70**, 094011 (2004), hep-ph/0405153.
- [51] K. Melnikov and A. Vainshtein, Phys. Rev. **D70**, 113006 (2004), hep-ph/0312226.
- [52] A. E. Dorokhov and W. Broniowski, Phys. Rev. **D78**, 073011 (2008), 0805.0760.

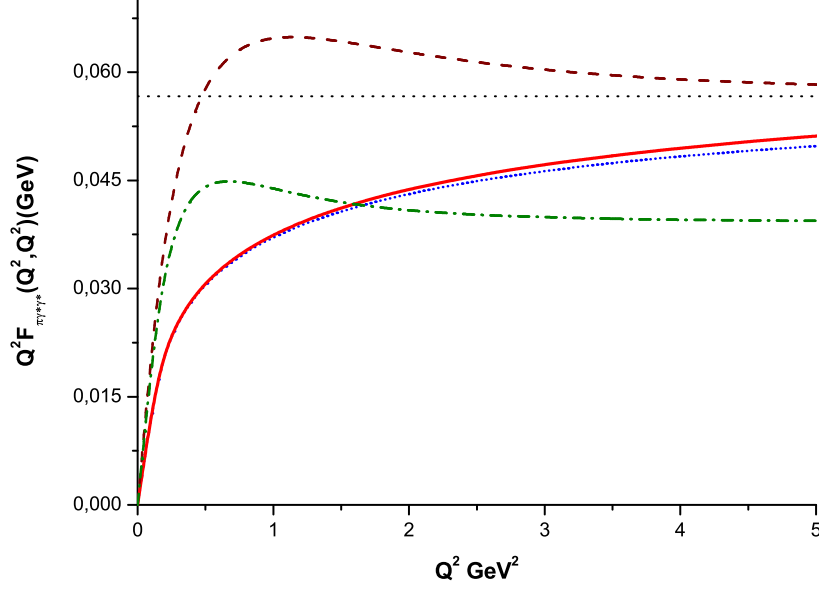


FIG. 7. Photon-pion transition form factor in symmetric kinematics for the instanton model with parameters $M_q = 125$ MeV, $\Lambda = 0.016$ GeV^{-2} (short pointed line), $M_q = 300$ MeV, $\Lambda = 1.3$ GeV^{-2} (dash-dotted line); and chiral model with parameters $M_q = 125$ MeV, $\Lambda = 0.0098$ GeV^{-2} (solid line) and $M_q = 300$ MeV, $\Lambda = 0.639$ GeV^{-2} (dashed line). The straight dotted line is asymptotic limit $2f_\pi/3$.

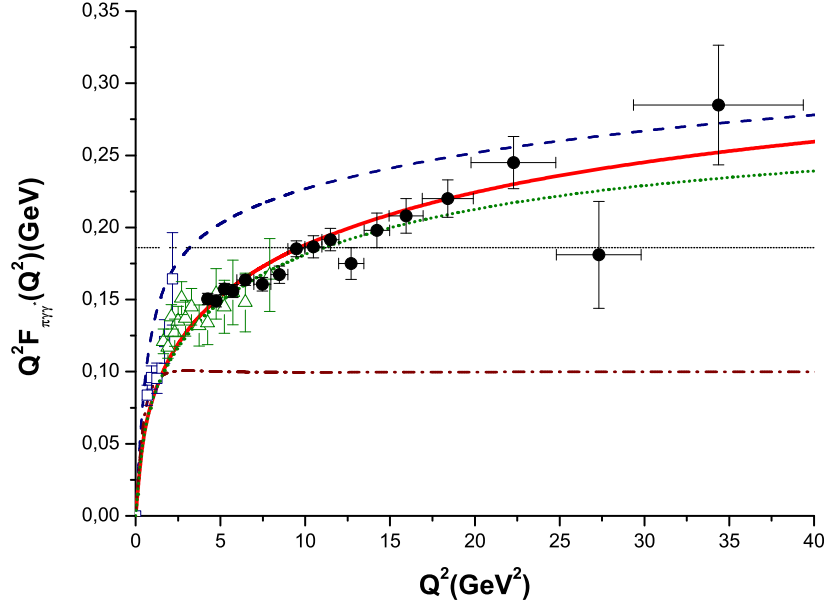


FIG. 8. Photon-pion transition form factor in asymmetric kinematics for the instanton model with parameters $M_q = 125$ MeV, $\Lambda = 0.016$ GeV^{-2} (short pointed line), $M_q = 300$ MeV, $\Lambda = 1.3$ GeV^{-2} (dash-dotted line); and chiral model with parameters $M_q = 125$ MeV, $\Lambda = 0.0098$ GeV^{-2} (solid line) and $M_q = 300$ MeV, $\Lambda = 0.639$ GeV^{-2} (dashed line). The straight dotted line is asymptotic limit $2f_\pi$.

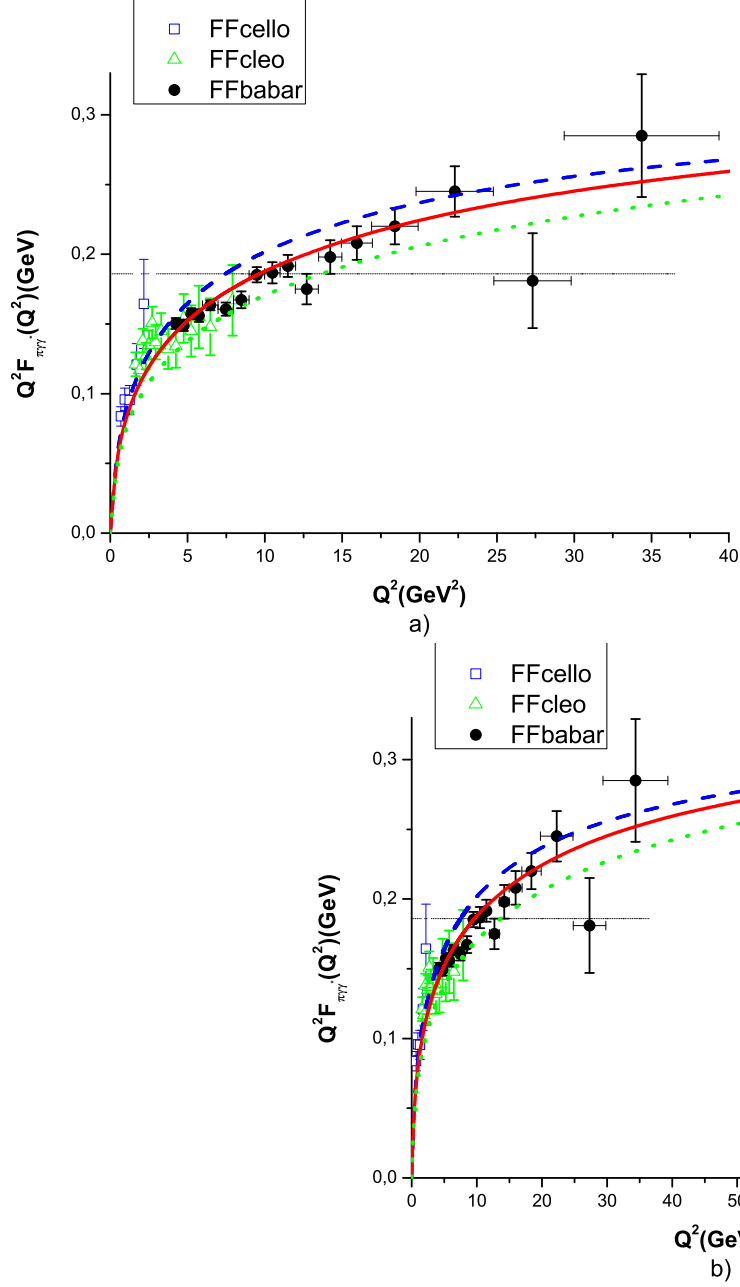


FIG. 9. Photon-pion transition form factor in asymmetric kinematics for the chiral model with parameters $M_q = 125$ MeV, $\Lambda = 0.0098$ GeV^{-2} (solid line), $M_q = 135$ MeV, $\Lambda = 0.0203$ GeV^{-2} (dashed line), $M_q = 115$ MeV, $\Lambda = 0.0038$ GeV^{-2} (dotted line). The straight dotted line is asymptotic limit $2f_\pi$.

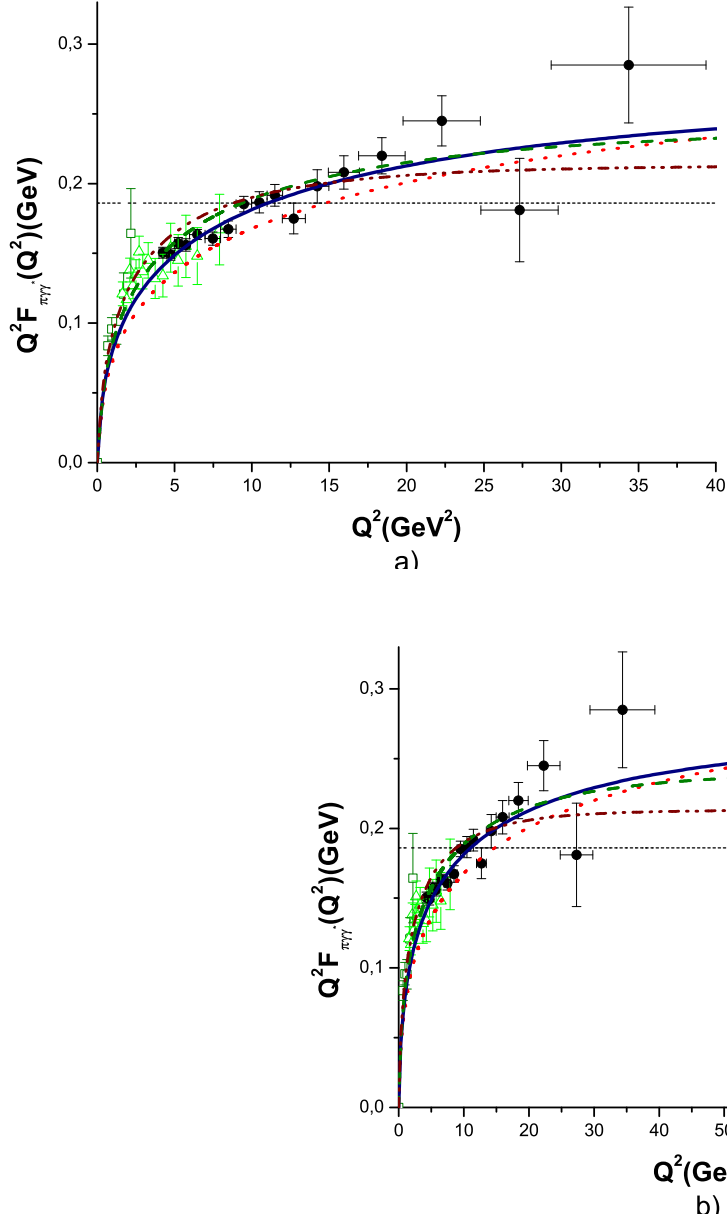


FIG. 10. Photon-pion transition form factor in asymmetric kinematics for the instanton model with parameters $M_q = 115$ MeV, $\Lambda = 0.0038$ GeV $^{-2}$ (dotted line), $M_q = 125$ MeV, $\Lambda = 0.0098$ GeV $^{-2}$ (solid line), $M_q = 135$ MeV, $\Lambda = 0.0203$ GeV $^{-2}$ (dashed line), $M_q = 150$ MeV, $\Lambda = 0.077$ GeV $^{-2}$ (dash-dot-dotted line). The straight dotted line is asymptotic limit $2f_\pi$.

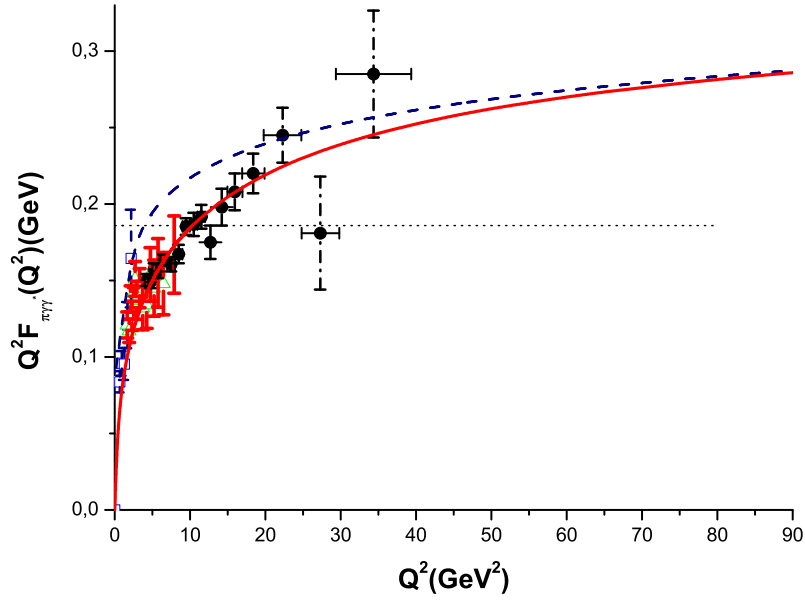


FIG. 11. Photon-pion transition form factor (solid line) and its asymptotic part (dashed line) in asymmetric kinematics for the chiral model with parameters $M_q = 125$ MeV, $\Lambda = 0.0098$ GeV^{-2} .